Journal of Mechanical Engineering Research and Developments
ISSN: 1024-1752
CODEN: JERDFO
Vol. 43, No. 2, pp. 336-342
Published Year 2020

Investigation of The Filler-Shape Effect on The Hydrophobicity and Transparency of Multilayer Nanocomposite Coating

Ammar Emad Al-kawaz[†], Firas J. Hmood[‡], Zainab M. Mohmmed[†] & Ali Amer[†]

[†]Faculty of Materials Engineering / Department of Polymers and Petrochemical Industries, University of Babylon, Babylon, Iraq

[‡]Faculty of Materials Engineering /Department of Ceramics Engineering and Building Materials, University of Babylon, Babylon, Iraq

Email: firas.hmood@googlemail.com

ABSTRACT: Solar panels are very interesting devices for energy harvesting. Self-cleaning coatings are necessary for the solar panels since rains and sand particles in dusty weather can damage the outer surfaces of the solar panels; in addition to lowering the energy harvested. Therefore, developing a special transparent and self-cleaning coating is of interest. In this work, transparent composite hydrophobic coatings of three layers was prepared using different coating techniques and investigated for hydrophobicity and optical transmittance. The first layer, which was of PMMA with a thickness of 200 µm, was coated by doctor blade technique. A second layer of different particles i.e. PTFE, TiO_2 and $CaSiO_3$ was spread out by dipping technique. Finally, a third layer, which was of pure PMMA with a thickness of around 10 nm, was coated by spin technique. A composite coating of PMMA / $CaSiO_3$ / PMMA shows a contact angle of around 129° which was the best performance among the prepared coatings. The results have also revealed that this coating can transmit up to 84% of the visible light at a surface roughness of 16 µm.

KEYWORDS: composite coating; contact angle; thin film; energy harvesting; roughness

INTRODUCTION

Hyper-hydrophobicity surfaces are very interesting in industry like self-cleaning glass windows and repellent surfaces for dust or ice [1-3]. Engineering of surfaces for high contact angle are achieved either by modifying the surface chemistry or by varying the surface features. Inducing functional groups to the surface material alters the surface chemistry. For instance, Tokuda et al. fluorinated PMMA surfaces by immersion the PMMA in a fluorinated reagent. The contact angle of water on the PMMA increased from 70° to 111° after fluorination [4]. Altering just the surface chemistry does not convert a surface from hydrophobic into superhydrophobic. Surface roughness should be changed on the micro- or nanolevel as well. As a result, this will lead to lower the free energy of surfaces [5]. Lowering the surface free energy will lead to increase lubricity, biocompatibility, and chemical durability. While increasing the surface free energy can lead to superhydrophobic surfaces [6]. According to the literature, engineering of surface features can be made by more than one method. Chemical etching or etching with plasma are effective to create controlled roughness [7,8]. While evaporation of some active groups like CO_2 leads to create nanoroughness [9-11]. Increasing of surface roughness leads to decrease the contact areas between the surface and the other materials which reduces the adhesion of precipitants to the surface. This belongs to the air entrapped within the cusps of the rough surface.

Different mathematical models describe how the contact angle can differ with the surface features. Figure 1 exhibits three models to evaluate the contact angle on different surface topologies. For homogeneous and smooth surface of one material, the equation of Young may be employed. It describes the contact angle on a flat smooth surface as following [12]:

$$\gamma_{SG} = \gamma_{SL} + \gamma_{LG}\cos\theta \quad (1)$$

θ is the contact angle for smooth surface, $\gamma_{SG}, \gamma_{SL}, \gamma_{LG}$ are solid-gas, solid-liquid, and liquid-gas interfacial tension, respectively.

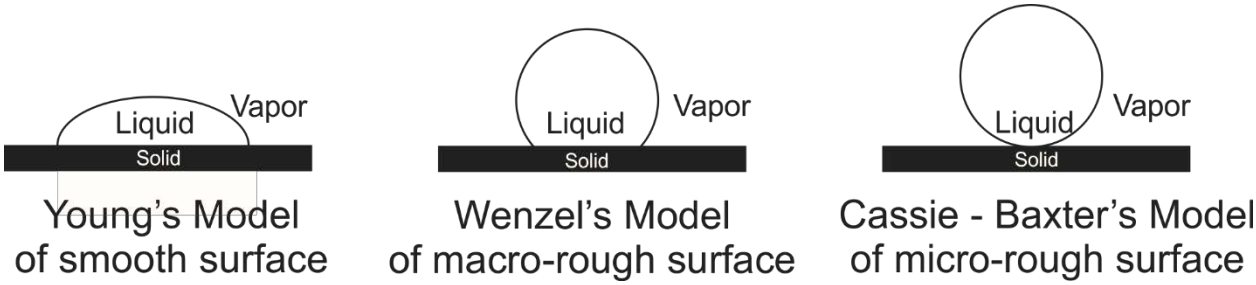

Figure 1. Effect of surface roughness on the contact angle of water droplet

This equation has been modified by Wenzel to include the effect of surface roughness on the wettability of surfaces (equation 2). He assumes that the microscopic flutings of a rough surface are filled with water droplets. This increases the actual shared area between liquid and surface resulting in lowering the contact angle (Figure 1b).

$$\cos\theta_w = \frac{r(\gamma_{SV}-\gamma_{SL})}{\gamma_{LV}} = r\cos\theta \quad (2)$$

Where θ_W: the apparent contact angle (Wenzel's angle), θ is the Young's angle and (r) is the factor of roughness. This factor is a fraction of actual surface area to the projected area. Therefore, the surface free energy of rough surface is times higher than that of a flat surface. For the heterogeneous surfaces consist of two different materials, Cassie and Baxter [6] suggested equation 3 to describe the contact angle θ as following:

$$\cos\theta = f\cos\theta + f - 1 \quad (3)$$

The letter f is the area of the solid-liquid interface and the term (1- f) is the area portion of the solid-air interface. This equation describes a regime where there is sufficient roughness for air trapping in peaks between the solid and liquid to form a composite interface.

Scientists have developed more than one method to mimic the superhydrophobicity of natural surfaces of some plants like lotus [13, 14]. For instance, artificial templates are used to generate controlled surface roughness. William et al. synthesized large-scale and low-cost coatings. The yield coatings appeared good anti-abrasion resistance, superhydrophobic in water droplet test and a lotus effect with sliding angles below 10° for up to 120° continuous abrasion cycles [15]. Electrospraying method has employed to prepare self-cleaning superhydrophobic surface with high transparency using an organosilane-coated alumina precursor. With such technique, spraying time influences resulting roughness and transparency [16]. The drawbacks of above-mentioned methods are cost and time consuming. An alternative method to make roughness is by adding organic or inorganic fillers. It is considered simple, cheap and easy to handle. Different fillers can be used to satisfy the surface requirements. Some of them can be treated superficially to high performance. Clay or silica particles, for instance, are used as filler for coatings either treated or not treated [17]. While others such as ZrO_2, TiO_2, etc. are used for this purpose without treated. Morrissette et at. declared that such ceramic fillers are not biodegradable and nontoxic; therefore, they do not harm the environment [18]. For optical applications this method suppose that the size of the additives must be small enough to allow the light to pass through without distortion. In this study we report about an easy method to prepare multi-layered polymer-based composite coatings with organic and inorganic particles as fillers. The goal of this work is to show the effect of different filler particles on the surface roughness and the contact angle of water considering the transparency of the resulting coatings.

EXPERIMENTS

Starting materials

The polymers that used in this work are polymethlemethacrylate (PMMA) as grains (d50: 2 mm) produced by sigma-Aldrich (molecular weight is 100.12 g/mol and density 1.18 g/cm). Poly(tetrafluoroethylene) (PTFE) (sigma-Aldrich, molecular weight of 100.02) was used as a powder with particle size of 35 μm. Nanoparticles of TiO_2 (anatas phase) with a particle size of 10 nm. Another powder was involved in this study which is Wollastonite and has an aspect ratio of 20:1. These powders were used to develop roughness on the outer surface of the proposed coating.

METHODOLOGY

Different coating solutions were prepared as following: 0.9 g from PMMA was dissolved in (9 ml) of Tetrahydroferan (THF) solvent. This mixture was used for the first and the third layers. Next, 0.25 wt% of each powder, i.e. PTFE, TiO_2 and $CaSiO_3$, were dispersed in THF. They were sonicated for 1 h at room temperature to destroy any agglomerated particles. Soad-lime glass was supplied as substrates (50 x 50 x 1.5 mm), which they well-cleaned by THF before coating. The first coating was deposited by the doctor blade technique. The second layer was spread out by dipping technique. Finally, the third layer was deposited by using the spinning technique. Figure 2 exhibits the consequence of the deposited layers. The thickness of the first was adjusted to 200 µm while the second layer was around 50 nm. The third was determined to 10 nm. The coating parameters have been well controlled to keep the thickness of the deposited layers equal.

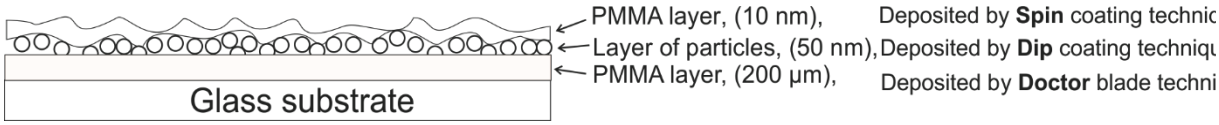

Figure 2. Sequence of layers of the composite coatings

Characterizations

Particle size distribution

Particle size of the starting powders was determined using a particle size analyser (Bettersize 2000, China). It can measure particle size from 0.002 nm to 2 mm.

Contact angle measurement

The contact angle was measured using an optical contact angle and interface tension meter (kion, SL200KS, china). Water drop was employed as a testing liquid.

Optical transmission

The optical transmission was measured using a UV-Viable spectrometer (UV-1800 Shimadzu) range from (190 - 1100 nm) used to get absorbance, transmittance, and reflectance and other optical properties of the films.

Roughness determination

The surface roughness of the developed composite coatings was determined using an atomic force spectroscopy (AA3000SPM, Angstrom Advanced Inc., USA).

RESULTS AND DISCUSSION

Contact angle (θ) is an indicator for surface hydrophobicity. If it is lower than 90°, surfaces exhibit hydrophilic tendency. On the other hand, if it is higher than 90°, surfaces are considered hydrophobic. Figure 3 shows variation in the static contact angles of water droplet onto different coatings. It shows that PMMA layer alone has a value of static contact angle of 77°. The contact angle of the third PMMA layer has varied according to the second layer of powders. For the sequence of PMMA / TiO_2 / PMMA, θ was increased from 77° to 95°. While the contact angle of the second layers order (PMMA / PTFE / PMMA) has increased from 77° to 98°. In the third layers sequence (PMMA / $CaSiO_3$ / PMMA), θ has increased up to 129°.

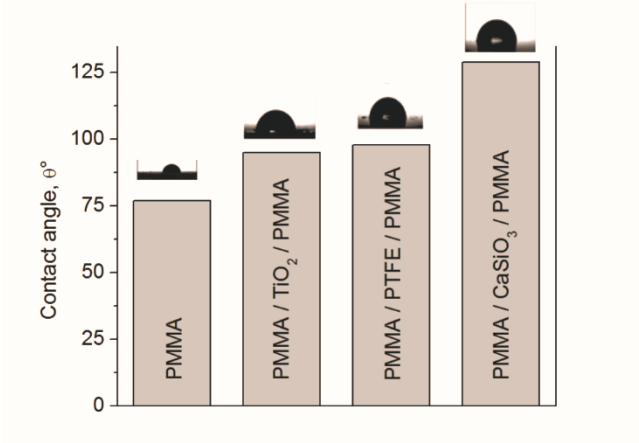

Figure 3. Static contact angle (θ) on different coating compositions

The added particles have changed the final outer roughness and it has varied according to the added material. Figure 3 also shows that the water drop on the TiO_2 filled composite coating has slightly lower contact area in comparison to that of PTFE filled coating. Considering the roughness, the crystals of anatas (TiO_2) and wollastonite are dissimilar. Anatas titania has a cubic structure while wollastonite has needle-like structure with an aspect ratio of 20:1. Therefore, the roughness comes from wollastonite particles is much higher than that of titania and PTFE. This, of course, will lead to raise the contact angle to higher values as a result of trapping air between the wollastonite cusps. It has been assumed that the particles distribution are uniform and the agglomerations are as low as possible over the entire coated area. Figure 4 exhibits that the roughness of the sequence (PMMA / CaSiO3 / PMMA) is approximately uniform with an average value of about 16 µm. The coating parameters have been well controlled (temperature, time, and the coating flowability) to keep the thickness of the deposited layers equal.

The optical transmittance of the coatings are shown in Figure 5. It exhibits that all the prepared coatings has an absorption at the UV range as a result of the polymer bonds. Introducing the filling powders has an effect on the UV absorption percentage.

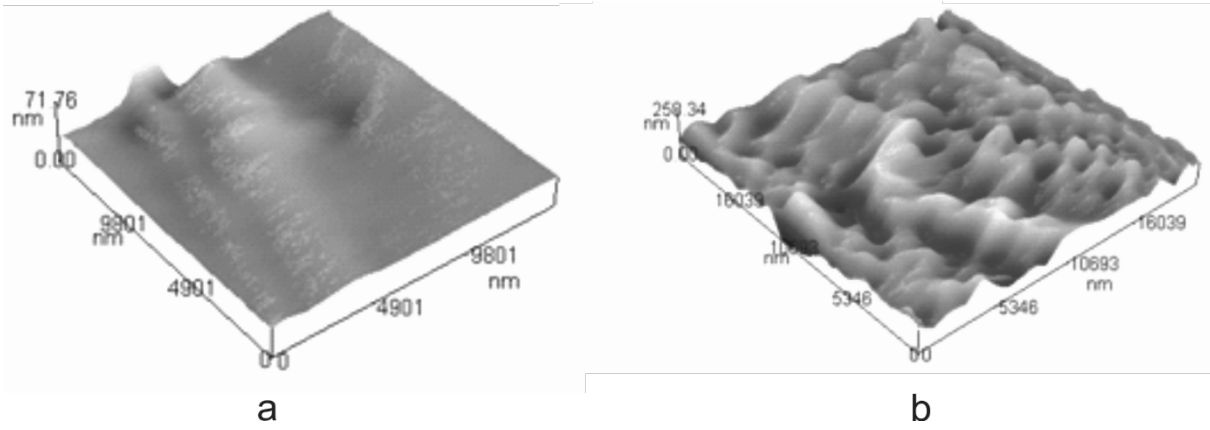

Figure 4. AFM images of coating surfaces a) pure PMMA and b) composite coating of three layers: PMMA / $CaSiO_3$ / PMMA

The order of PMMA / $CaSiO_3$ / PMMA shows the lowest UV absorption of about 10%. PMMA / PTFE / PMMA coating has an UV absorption of around 15%. While involving the TiO_2 has increased the absorption up to 25%. Increasing the wavelength more than 300 nm has led to increase the optical transmittance especially at the visible light. This indicates that the light transmission has varied according to the additives and their distribution over the whole coating area which is related to the yield outer surface roughness.

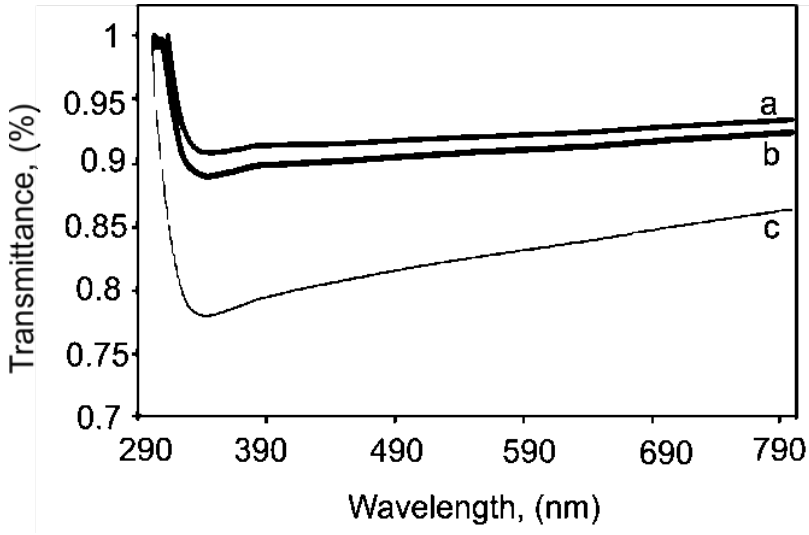

Figure 5. Optical transmittance behaviour for different types of coating; a) PMMA / TiO_2 / PMMA; b) PMMA / PTFE / PMMA; c) PMMA / $CaSiO_3$ /PMMA.

Table 1 sums up the results of all the synthesised coatings which include the contact angle, surface roughness and the optical transmittance at the visible light (wavelength 600 nm). In fact, since the base material (PMMA) properties was not chemically modified, the resulting roughness generated by titania, PTFE and wollastonite particles is the main effect that has varied the hydrophobicity of the coatings.

Table 1. Values of surface roughness and optical transmittance for different coatings

Sample	Contact angle, θ°	Surface roughness, µm	Transmittance at the visible light, %
PMMA / $CaSiO_3$ / PMMA	129	16	84
PMMA / PTFE / PMMA	97	10	90
PMMA / TiO_2 / PMMA	95	8	93

Decreasing the optical transmittance can return to the distribution of the titania and wollastonite particles which may be heterogeneous. Alternatively, the final polymer layer (PMMA) has increased the distortion centres of light of the coatings by increasing the surface roughness in addition to the fillers. In fact, it is not easy to combine both superhydrophobicity and visible light transmittance. Because increasing the roughness leads to increase Mie and Rayleih scattering of the incident light beam where both of them depend upon the roughness scale against the wavelength of the incident light [19]. Another factor that has huge influence of the light transmittance is the thickness of the deposited coating which is directly proportional to the layer thickness. It has been assumed to be equal but this cannot be true, since the coating process manually runs. However, the coating parameters have been well controlled to keep the thickness of the deposited layers equal. Speaking about layers interfaces and their influence on the light transmission was out of the work scope.

CONCLUSIONS

This research focuses on developing hydrophobic and transparent coatings. Multi-layer composite coatings was prepared using doctor bled and dip coating methods. The results of the static contact angle revealed that final surface roughness has raised the contact angle of PMMA up to 129° by adding $CaSiO_3$. Moreover, the created roughness has decreased the transparency of the yield coating as a result of light scattering and distortion at the interfaces as well as at the rough outer surfaces. In the future we will try to prepare surfaces that have ability to repeal dust.

ACKNOWLEDGMENTS

The authors would like to thank Mrs. Ibtissam at the department of ceramics engineering and building materials

- university of Babylon for making the contact angle measurements. Funding: This work was achieved without any financial support from any institution or organization.

REFERENCES

[1] A. Rifaia, N. Abu-Dheira, M. Khaledb, N. Al-Aqeelia, B. Sami Yilbasa. "Characteristics of oil impregnated hydrophobic glass surfaces in relation to self-cleaning of environmental dust particles". *Solar Energy Materials and Solar Cells*, vol. 171, pp. 8–15, 2017.

[2] B.P. Jellea, T. Gaoa, S.A. Mofida, T. Kolåsc, P.M. Stenstadd, S. Ng. "Avoiding Snow and Ice Formation on Exterior Solar Cell Surfaces: A Review of Research Pathways and Opportunities". *Procedia Engineering*, vol. 145, pp. 699–706, 2016.

[3] I. Yilgor, S. Bilgin, M. Isik, E. Yilgor. "Facile preparation of superhydrophobic polymer surfaces". *Polymer* (Guildf), vol. 53, pp. 1180–1188, 2012.

[4] K. Tokuda, T. Ogino, M. Kotera, T. Nishino. "Simple method for lowering poly (methyl methacrylate) surface energy with fluorination". *Polymer J.*, vol. 47, pp. 66–70, 2015.

[5] Q. Zheng, C. Lü. "Size effects of surface roughness to superhydrophobicity". Procedia IUTAM, vol. 10, pp. 462–475, 2014.

[6] Z. Yoshimitsu, A. Nakajima, T. Watanabe. "Effects of Surface Structure on the Hydrophobicity and Sliding Behavior of Water Droplets". *Langmuir*, vol. 18, pp. 5818–5822, 2002.

[7] L. Li, V. Breedveld, D.W. Hess. "Creation of superhydrophobic stainless steel surfaces by acid treatments and hydrophobic film deposition". ACS Appl. Mater. *Interfaces*, vol. 4, pp. 4549–4556, 2012.

[8] M. Martin, G. Cunge. "Surface roughness generated by plasma etching processes of silicon". *J. Vac. Sci. Technol. B*, vol. 26, pp. 1281–1288, 2008.

[9] G.H. Brink, N. Foley, D. Zwaan, J.B. Kooi, G. Palasantzas. "Roughness controlled superhydrophobicity on single nanometer length scale with metal nanoparticles". *RSC Adv.*, vol. 5, pp. 28696–28702, 2015.

[10] X. Wang, X. Li, Q. Lei, Y. Wu, W. Li. "Fabrication of superhydrophobic composite coating based on fluorosilicone resin and silica nanoparticles". *Soc. open sci.*, vol. 5, pp. 180598, 2018.

[11] N. Okulova, P. Johansen, L. Christensen, R. Taboryski. "Effect of structure hierarchy for superhydrophobic polymer surfaces studied by droplet evaporation". *Nanomaterials*, vol. 8, pp. 831, 2018.

[12] D. Zhang, L. Wang, H. Qian, X. Li. "Superhydrophobic surfaces for corrosion protection : a review of recent progresses and future directions". *J Coat Technol Res.*, vol. 13, pp. 11–29, 2016.

[13] S.S. Latthe, C. Terashima, K. Nakata, A. Fujishima. "Superhydrophobic Surfaces Developed by Mimicking Hierarchical Surface Morphology of Lotus Leaf". *Molecules*, vol. 19, pp. 4256–4283, 2014.

[14] D. Quere, M. Reyssat. "Non-adhesive lotus and other hydrophobic materials". *Phil. Trans. R. Soc.*, A vol. 366, pp. 1539–1556, 2008.

[15] W.S.Y. Wong, Z.H. Stachurski, D.R. Nisbet, A. Tricoli. "Ultra-Durable and Transparent Self-Cleaning Surfaces by Large-Scale Self-Assembly of Hierarchical Interpenetrated Polymer Networks". *ACS Appl. Mater. Interfaces.*, vol. 8, pp. 13615–13623, 2016.

[16] H. Yoon, H. Kim, S.S. Latthe, M. Kim, S. Al-deyab, S.S. Yoon. 2015. "A highly transparent self-cleaning superhydrophobic surface by organosilane-coated alumina particles deposited via electrospraying". *J. Mater. Chem. A.*, vol. 3, pp. 11403–11410.

[17] M. Joshi, A. Bhattacharyya, N. Agarwal, S. Parmar. "Nanostructured coatings for super hydrophobic textiles". *Bull. Mater. Sci.*, vol. 35, pp. 933–938, 2012.

[18] C. Xue, J. Ma. “Long-lived superhydrophobic surfaces”. *J. Mater. Chem. A*, vol. 1, pp. 4146–4161, 2013.

[19] R.G. Karunakaran, C.H. Lu, Z.H. Zhang, S. Yang. “Highly transparent superhydrophobic surfaces from the coassembly of nanoparticles (<= 100 nm)”. *Langmuir*, vol. 27, pp. 4594–4602, 2011.